

## Modelling of the process of adsorption of nickel in bentonite clay

Vieira, M. G. A.<sup>1</sup>, Gimenes, M. L.<sup>2</sup> and da Silva, M. G. C.<sup>3\*</sup>

<sup>1,3</sup> UNICAMP/FEQ/DTF; <sup>2</sup>UEM/CTC/DEQ

\*UNICAMP/FEQ/DTF, P.Box: 6066, Zip Code: 13083-970 Campinas – SP - Brazil

E-mail: meuris@feq.unicamp.br, F. 55 19 35213928 - Fax: 55 19 35213922

The bentonite clays have presented good adsorptive characteristics, being used as adsorbent alternative in the removal of heavy metals. This study aimed at studying the process of removal of nickel by Bofe calcined clay in porous bed. A study was conducted to select the operating flow rate, based on the smallest mass transfer zone (MTZ), on useful ( $q_U$ ) and total adsorbed ( $q_T$ ) removal quantities and on the percentage of total nickel removal (% Rem). The results were adjusted to the model corresponding to the Logistic function available in the *Origin* 6.1 software, with an excellent experimental model adsorption adjustment to date. The modelling allowed the selection of a function that describes the behavior of nickel adsorption in Bofe clay considering the experimental data of the rupture curves. The chemical composition of the calcined clay was characterized by EDX, N<sub>2</sub> Fisisorption and He picnometry.

### 1. Introduction

The use of clays for the adsorption or removal of heavy metals found in wastewater has recently been the object of study in many researches due to innumerable economical advantages (Ouhadi *et al.*, 2006; Novakovic *et al.*, 2008, Stathi *et al.*, 2007). The cost of clays is relatively low in comparison to other alternative adsorbents. Clays and minerals such as montmorillonite, vermiculite, illite, kaolinite and bentonite are among those natural materials which have been investigated as heavy metal adsorbents (Bhattacharyya and Gupta, 2008). Another advantage of using clay as adsorbent resides in its intrinsic properties, such as high specific surface area, excellent physical and chemical stability, and several other structural and surface properties (Chen *et al.*, 2008). Mathematical models and computational techniques are helpful in the identification of the phenomena involved in the process, in the equilibrium data analysis and interpretation, in the prediction of answers to changes in operation conditions, and in the optimization of processes. The heavy metal adsorption process models and computational simulation are important tools, as they make technology transfer possible by means of scale enlargement.

This study evaluated nickel removal by Bofe calcined clay in porous bed. A study was conducted in order to select the operating flow rate, based on the smallest mass transfer

zone (MTZ), on useful ( $q_U$ ) and total ( $q_T$ ) removal quantities adsorbed and on the percentage of total nickel removal (% Rem).

## 2. Material and Method

### 2.1 Clay adsorbent

Bofe bentonite clay proceeding from the Northeastern region of Brazil was used. The clay was ground, sifted, and classified according to the granulometry suitable for the use in porous bed column. Next, the clay was calcined in a muffle furnace at 500°C for 24 hours.

The chemical composition (% molecular) attained by EDX corresponds to 46.17% Si, 6.84% Al, 3.32% Fe, 1.19% Mg, 0.53% Ti, 0.58% Ca and 0.50% Na. The area attained by the BET method was 89.02 m<sup>2</sup>.g<sup>-1</sup>, with a volume of micropores and mesopores equivalent to 21.66 and 31.94 cm<sup>3</sup>/g, respectively. The clay's real density attained by Helium picnometry is of 2.4866 g/cm<sup>3</sup>.

### 2.2 Adsorption experiments

Adsorption experiments were developed in a porous bed system composed of a fourteen-centimeter long acrylic column, with an internal diameter of 1.4 cm, filled with clay with a mean diameter of 0.855 mm, and the fluid fed by a peristaltic pump. The tests were carried out with a monocomponent nickel solution at a concentration of 50 ppm (0.85 mM). The nickel concentration found in the solutions' liquid phase was determined by Atomic Absorption Spectrophotometer.

### 2.3 Calculation of MTZ, $q_U$ , $q_T$ and Percentage removal

The column's useful and total removal capacities correspond, respectively, to the metal removal up to the rupture point ( $q_U$ ) and saturation ( $q_T$ ). Equations 1 and 2 were attained through mass balance in the column by using the column's saturation data, starting with its rupture curves, where the area from bellow the curve ( $1-C/C_0$ ) to the rupture point is proportional to  $q_U$  and to bed exhaustion proportional to  $q_T$ , according to Geankoplis's model (1993):

$$q_T = \frac{C_0 Q}{1000m} \int_0^{t_b} \left(1 - \frac{C|_{z=L}}{C_0}\right) dt \quad (1)$$

$$q_U = \frac{C_0 Q}{1000m} \int_0^{t_b} \left(1 - \frac{C|_{z=L}}{C_0}\right) dt \quad (2)$$

Being:  $q_T$  and  $q_U$ , the total and useful metal adsorption capacities (mg of metal/g of clay);  $m$ , the adsorbent's dry mass (g of clay);  $Q$ , the solution's volumetric flow (cm<sup>3</sup>/min);  $C|_{z=L}$  and  $C_0$ , the metal concentrations at the column's exit and entrance (ppm);  $t_b$ , the time until the rupture point (min); and  $t$ , the process time (min).

The MTZ may then be calculated by the ratio  $q_U/q_T$  according to Equation 3. This equation has a maximum value that corresponds to the bed's height ( $H_L$ ) and, as mass

transfer efficiency increases, this value drops to the ideal condition in which the MTZ would be null and the rupture curve a step-function. Therefore, while for some removal quantities the bigger the value, the more efficient the process; for the MTZ the smaller the value, the more efficient the process, being the latter dependent on the operational conditions.

$$MTZ = H_L \left( 1 - \frac{q_U}{q_T} \right) \quad (3)$$

The total removal percentage during adsorption was attained by considering the metal fraction in solution that was retained in the adsorbent solid from all wastewater used in the adsorption process until bed saturation occurred. By using the values of the initial concentration ( $C_0$ ), the volume of solution flowed during adsorption, and the quantity of metal removed ( $q_T$ ), the percentage removal can be determined (%Rem). The quantity of adsorbed metal is calculated through the curve area of  $(1 - C/C_0)$  versus  $t$  (Volesky *et al.*, 2003).

#### 2.4 Study of Flow

The choice of the most adequate flow for the removal of this metal in clay was made in accordance to the results attained from the analysis of the MTZ,  $q_U$ ,  $q_T$  and %Rem. Tests were carried out with flows of 4, 5, 6 and 8 mL/min, thus operating in laminar flow regimen (Darcyan).

#### 2.5 Process Modelling

The modelling through the Origin 6.1 software allows the selection of a function that describes the behavior of nickel adsorption in calcined Bofe clay regarding the experimental data of the rupture curves. Out of the adjustment functions available in the software, the *Logistic* function was selected according to Equation 4, for it presented a high nonlinear correlation coefficient ( $R^2$ ) and reproduced the experimental curve's behavior well.

$$y = \frac{A_1 - A_2}{1 + \left( \frac{x}{x_0} \right)^p} + A_2 \quad (4)$$

At each curve,  $A_2$  was used in the *Logistic* function as being equal to 1, that is, the value to which the end of the curve tends in  $C_i/C_0$ .  $A_1$  was chosen as being zero, representing the nickel concentration in the wastewater at the first instant. The *Logistic* function curve adjusted to the rupture data was attained for each flow.

### 3. Results

#### 3.1 Study of fixed-bed adsorption flow

Figure 1 shows the rupture curves for the different flows studied (4, 5, 6 and 8 mL/min), with *Logistic* function adjustments for the respective experimental data.

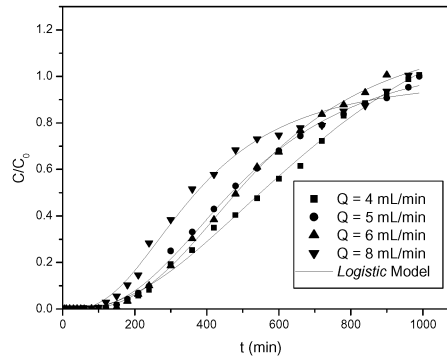


Figure 1: Breakthrough curves of nickel in Bofe clay adjusted by the Logistic function.

Figure 1 shows that the breakthrough curves presented distinct behaviors, indicating the influence of the flow on the diffusional resistances. The adsorption process shows, for the whole flow band studied, a strong resistance to bed saturation, which is confirmed by the longer rupture curves and the ample mass transfer zones. In Table 1, the values of the MTZ,  $q_U$ ,  $q_T$  and nickel removal percentage in Bofe clay are shown. It was also observed that the smallest MTZ and satisfactory  $q_U$ ,  $q_T$  and %Rem values were attained for the flow of 5 mL/min.

Table 1: MTZ,  $q_U$ ,  $q_T$  and %Rem values for nickel adsorption in Bofe clay.

Flow (mL/min)	MTZ (cm)	$q_U$ (mg/g)	$q_T$ (mg/g)	%Rem
4	10.04	1.65	5.84	65.75
5	8.64	2.30	6.00	51.28
6	8.77	2.32	6.20	52.96
8	9.83	2.35	7.90	42.00

### 3.2 Modelling of Nickel adsorption in Bofe clay

The values of  $X_0$  and  $p$  of the Logistic function adjusted to the rupture data attained for one of the flows studied are shown in Table 2.

Table 2: Logistic function's adjustment coefficient for the flows considered.

Flow (mL/min)	$X_0$	$p$	$R^2$
4	521.9930	3.5437	0.9866
5	464.3827	3.2496	0.9965
6	412.9737	3.0324	0.9994
8	319.0357	2.4283	0.9920

It was observed that the curve's adjustment coefficients are strongly dependent on the flow values. For this reason, each coefficient was separately plotted in relation to the flow. Linear adjustments for  $X_0$  ( $R^2 = 0.9977$ ) and  $p$  ( $R^2 = 0.9969$ ) were attained in relation to the flow. By adding the linear coefficients, Equations 5 and 6 are produced, which represent the behavior of coefficients  $X_0$  and  $p$ , respectively.

$$Y(X_0) = 719.1998 - 50.3658.x \quad (5)$$

$$Y(p) = 4.6474 - 0.27768.x \quad (6)$$

Equation 7 is attained by replacing the expressions found for  $x_0$  and  $p$ , Equations 5 and 6, respectively, in the Logistic model equation, Equation 4, and the correspondent variables.

$$\frac{C}{C_0} = \frac{A_1 - A_2}{1 + (t/x_0)^p} + A_2 \quad (7)$$

$$X_0 = 719.1998 - 50.3658.x$$

$$p = 4.6474 - 0.27768.x$$

$$A_1 = 0; A_2 = 1$$

From Equation 7, a numeric model is obtained which is capable of drawing a complete nickel adsorption rupture curve by means of an arbitrary selection of a flow value. Equation 7 was simulated by the Origin 6.1 software for the same flows used in the experiment in order to prove the efficiency of the model proposed, according to the modelling presented in Figure 2a. This model is valid only for the flow band studied. The adjustment efficiency can be verified through the behavior similarity between the experimental and simulated curves.

As shown in Figure 2a, the model correspondent to the *Logistic* function adequately represented the behavior of the complete nickel adsorption rupture curve for the flow band from 4 to 8 m/min. Through the function attained in Equation 7, rupture curves for the flows that were not experimentally performed can be simulated, such as 3, 7 and 9 mL/min, as shown in Figure 2b.

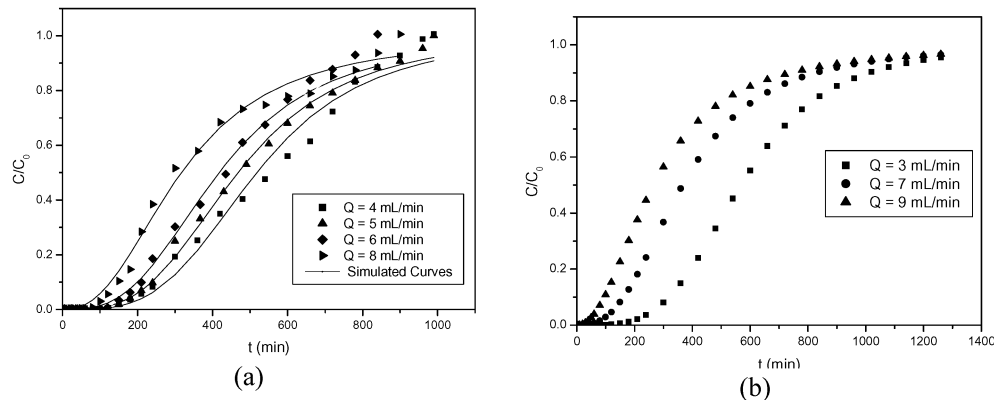


Figure 2: (a) Experimental breakthrough curves and their respective models; (b) Simulated breakthrough curves of nickel adsorption in clay.

Based on the simulated breakthrough curves, values of the MZT, useful and total removal quantities, and total percentage of nickel removal in Bofe clay were estimated, whose values can be found in Table 3.

Table 3: Estimated values of the MTZ,  $q_U$ ,  $q_T$  and %Rem for the simulated breakthrough curves of nickel adsorption in Bofe clay.

Flow (mL/min)	MTZ (cm)	$q_U$ (mg/g)	$q_T$ (mg/g)	%Rem
3	8.45	2.03	5.12	31.58
7	10.22	2.24	8.30	34.82
9	11.31	1.73	9.01	17.64

By comparing the estimated values with the experimental values presented in Table 1, it can be concluded that the flow of 5 mL/min is the most adequate operation flow in the entire flow band studied, that is, from 3 to 9 mL/min, given that the MTZ attained for this flow is very close to the minimum simulated for the flow of 3 mL/min, but with a removal percentage way superior to the estimated one.

#### 4. Conclusions

The fixed-bed adsorption process presented, for the flow band studied, a strong resistance to bed saturation, which was confirmed by the longer breakthrough curves and the ample mass transfer zones. Within the flow band studied, the 5 mL/min condition presented the smallest MTZ value (8.64 cm).

The modelling through the Origin 6.1 software allowed the attainment of a function (*Logistic*) which describes the behavior of nickel adsorption in calcined Bofe clay considering the experimental data of the breakthrough curves attained with other flows. Based on the function obtained, satisfactory breakthrough curves were simulated for the flows which were not experimentally performed.

#### 5. Acknowledgments

The authors acknowledge the financial support received from CNPq and FAPESP.

#### 6. References

- Bhattacharyya, K.G. and S.S. Gupta, 2008, Adsorption of a few heavy metals on natural and modified kaolinite and montmorillonite: A review. *Adv. Colloid Interface Sci.*, 140(2), 114-131.
- Chen, W.J., L.C. Hsiao and K.K.Y. Chen, 2008, Metal desorption from copper(II)/nickel(II)-spiked kaolin as a soil component using plant-derived saponin biosurfactant. *Process Biochem.*, 43(5), 488-498.
- Geankoplis, C. J., 1993, *Transport Process and Unit Operations*. 3<sup>a</sup> ed., PTR Prentice Hall, USA.
- Novakovic, T., L. Rozic, S. Petrovic and A. Rosic, 2008, Synthesis and characterization of acid-activated Serbian smectite clays obtained by statistically designed experiments. *Chem. Eng. J.*, 137(2), 436-442.
- Ouhadi, V.R., R.N. Yong and M. Sedighi, 2006, Desorption response and degradation of buffering capability of bentonite, subjected to heavy metal contaminants. *Eng. Geology*, 85(1-2), 102-110.
- Stathi, P., K. Litina, D. Gournis, T. S. Giannopoulos and Y. Deligiannakis, 2007, Physicochemical study of novel organoclays as heavy metal ion adsorbents for environmental remediation. *J. of Colloid and Interface Sci.*, 316(2), 298-309.
- Volesky, B., J. Weber and J.M. Park, 2003, Continuous-flow metal biosorption in a regenerable *Sargassum* column. *Water Research*, 297-306.